Electronic Supplementary Material (ESI) for RSC Advances.
This journal is © The Royal Society of Chemistry 2014

Supporting Information

A novel coumarin based molecular switch for dual sensing of Zn(II) and Cu(II)

Deblina Sarkar,[a] Ajoy Kumar Pramanik,[a] and Tapan Kumar Mondal[a]*

[a] *Department of Chemistry, Jadavpur University, Kolkata-700032, India E-mail: tkmondal@chemistry.jdvu.ac.in*

Contents

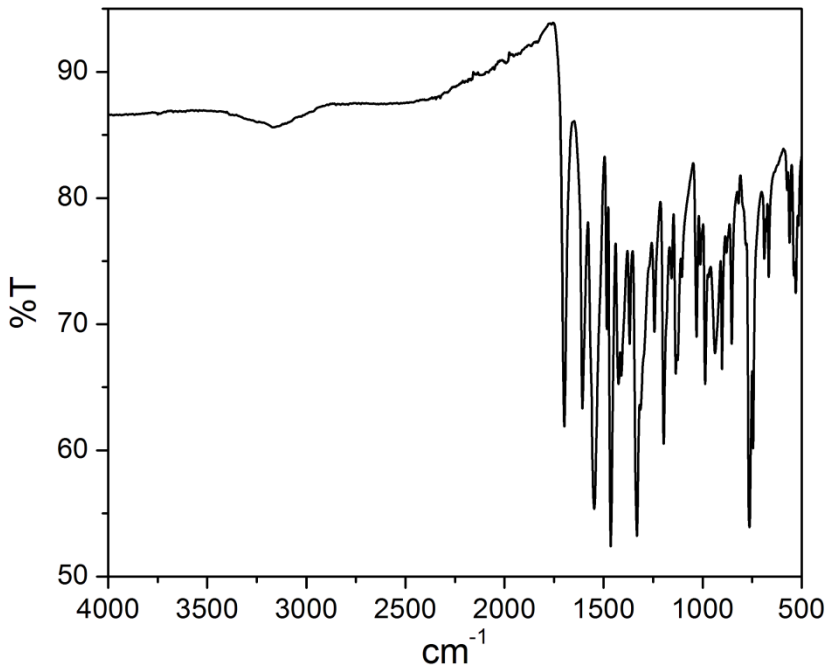

Fig. S1. IR spectrum of H_2L in KBr disk

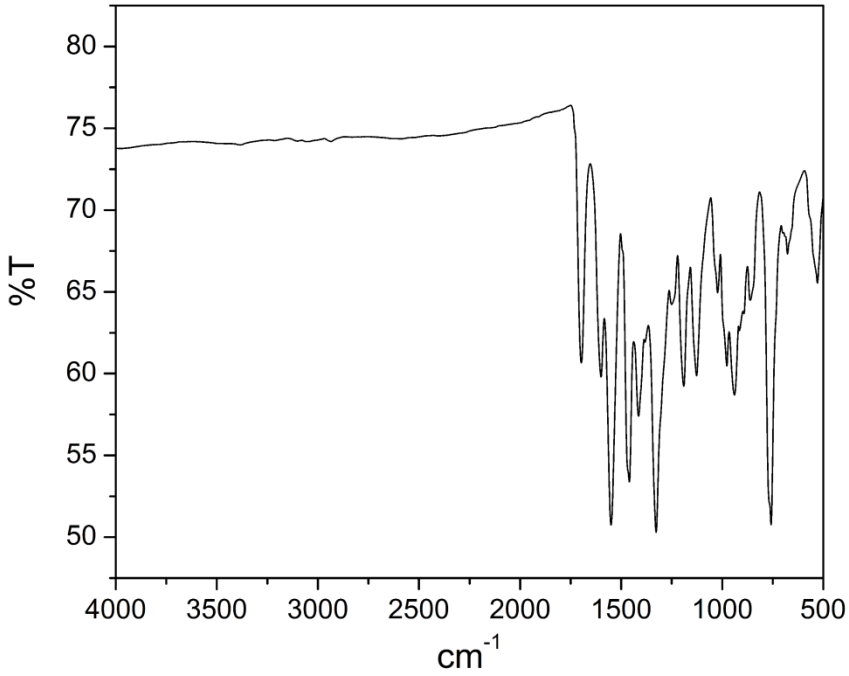

Fig. S2. IR spectrum of H_2L-Zn^{2+} in KBr disk

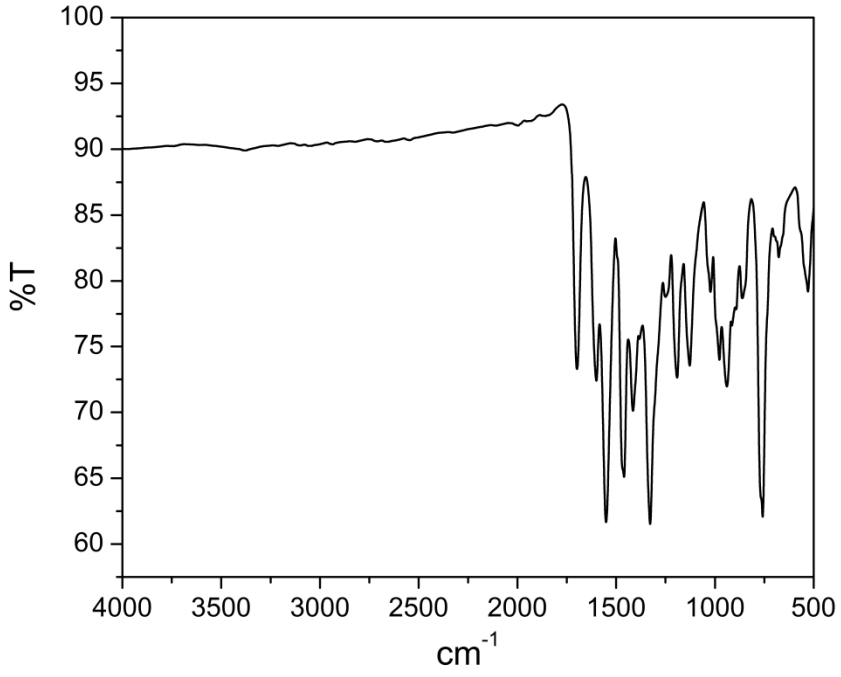

Fig. S3. IR spectrum of H_2L-Cu^{2+} in KBr disk

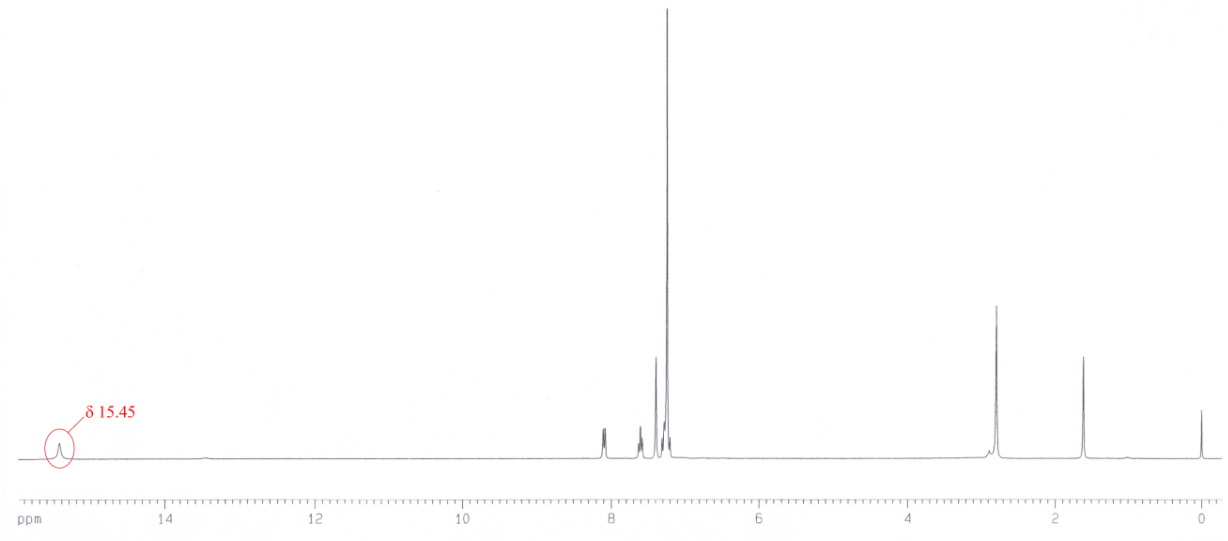

Fig. S4. ^{1}H-NMR spectra of H_2L in $CDCl_3$

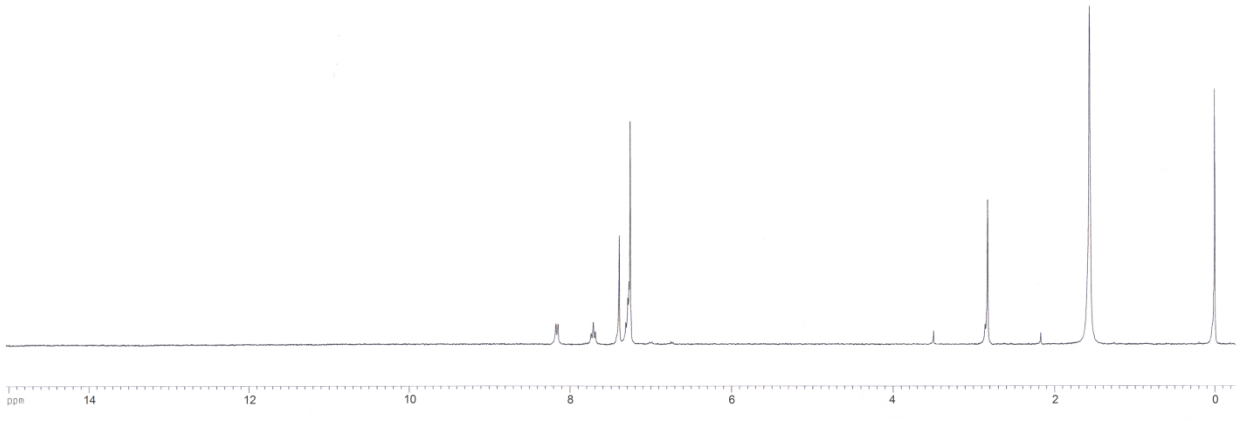

Fig. S5. ^{1}H-NMR spectra of H_2L-Zn^{2+} in $CDCl_3$

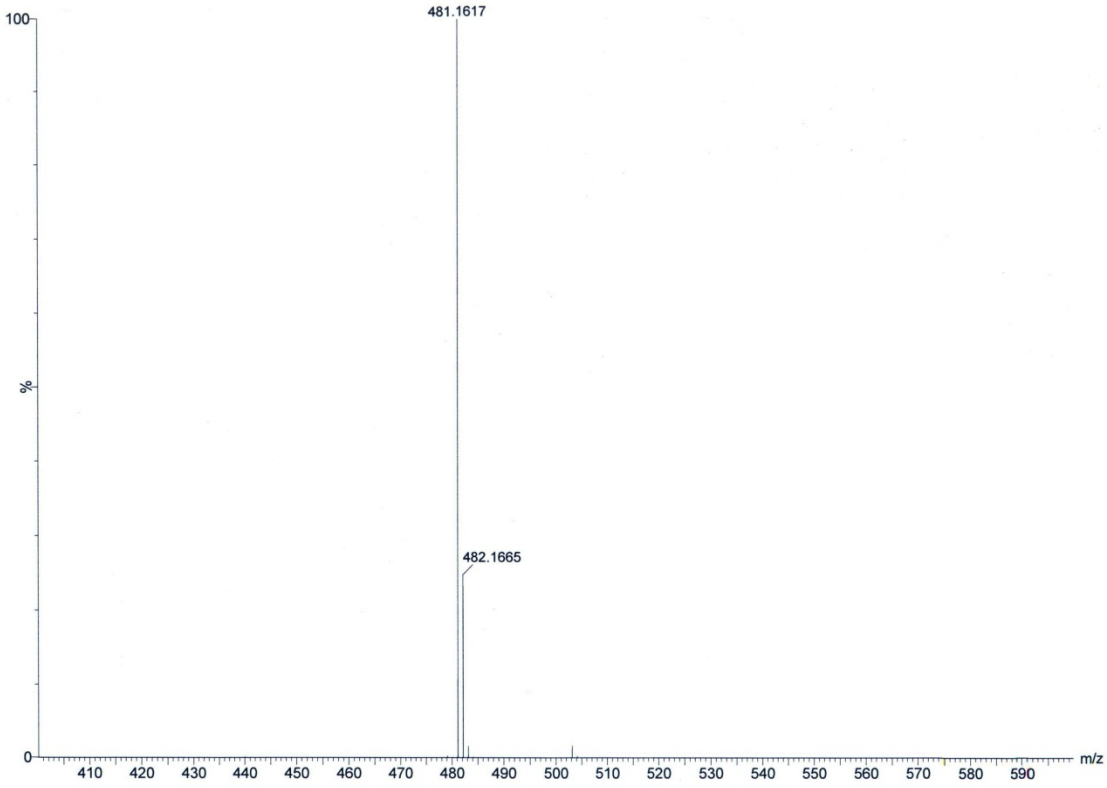

Fig. S6. HRMS spectra of the receptor H_2L

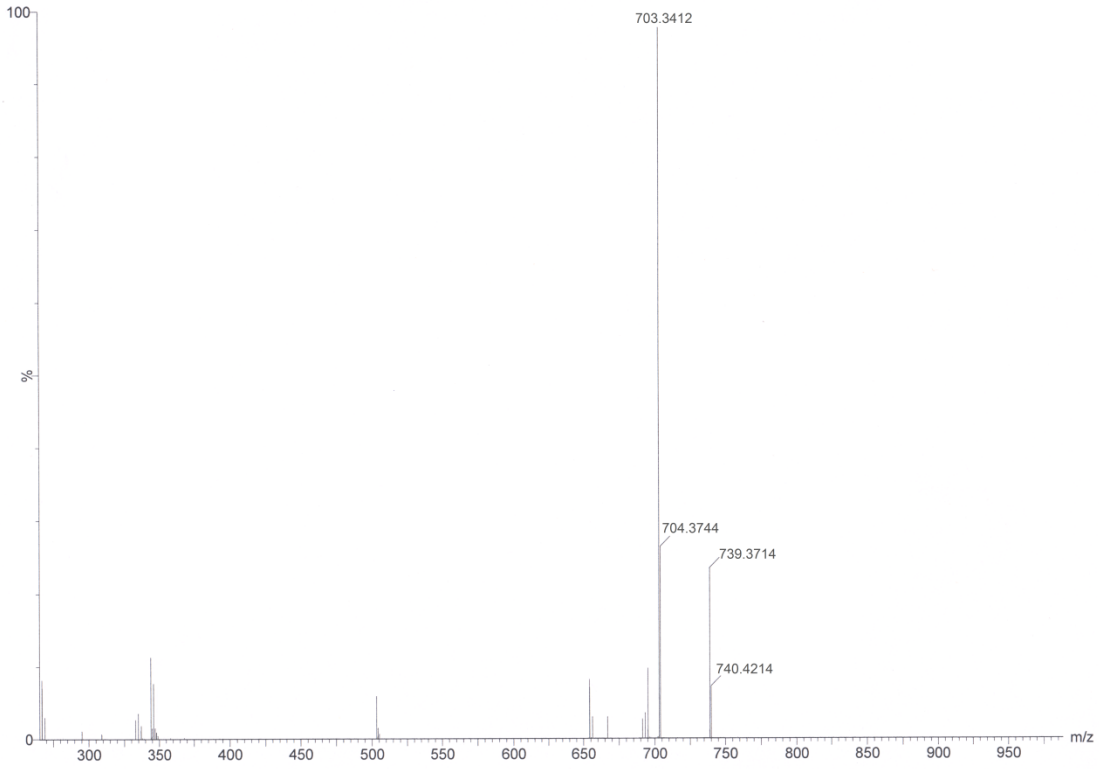

Fig. S7. HRMS spectra of the receptor H_2L-Zn^{2+} complex

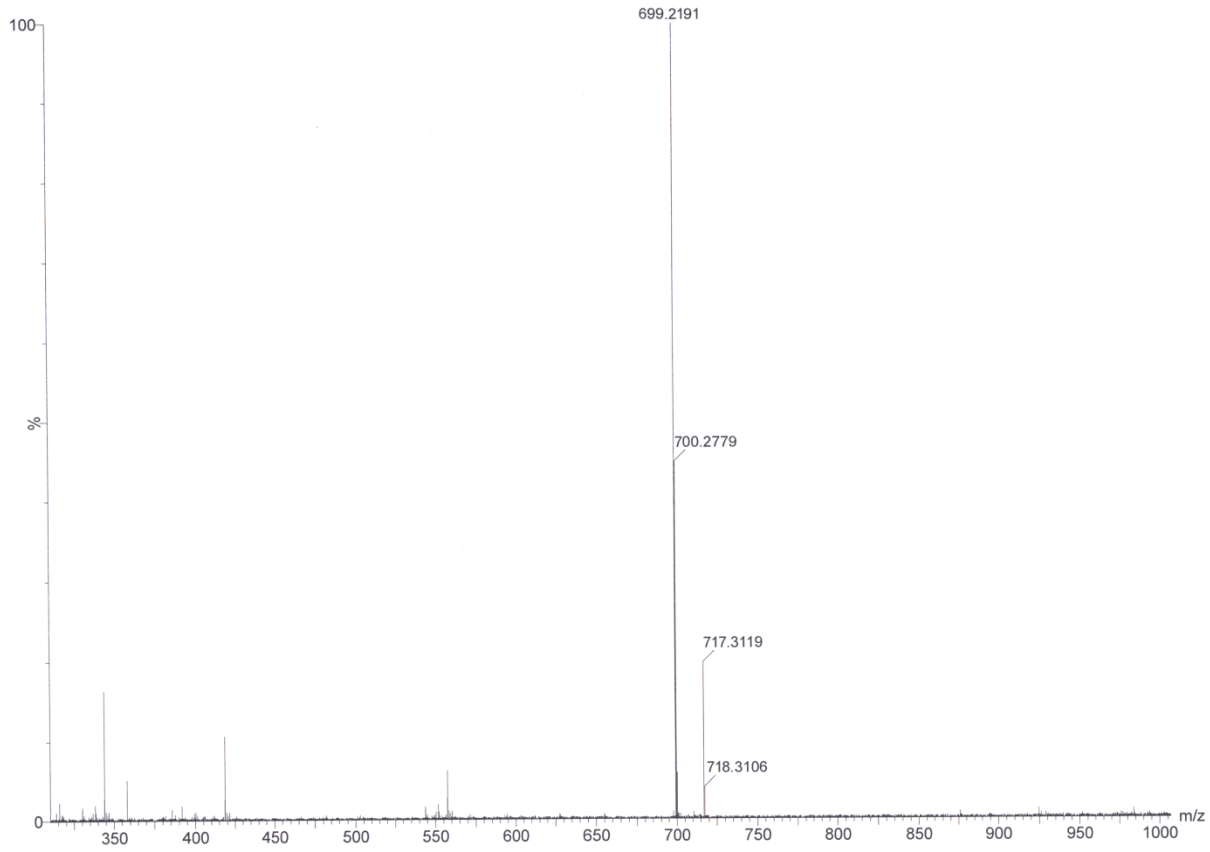

Fig. S8. HRMS spectra of the receptor H_2L-Cu^{2+} complex

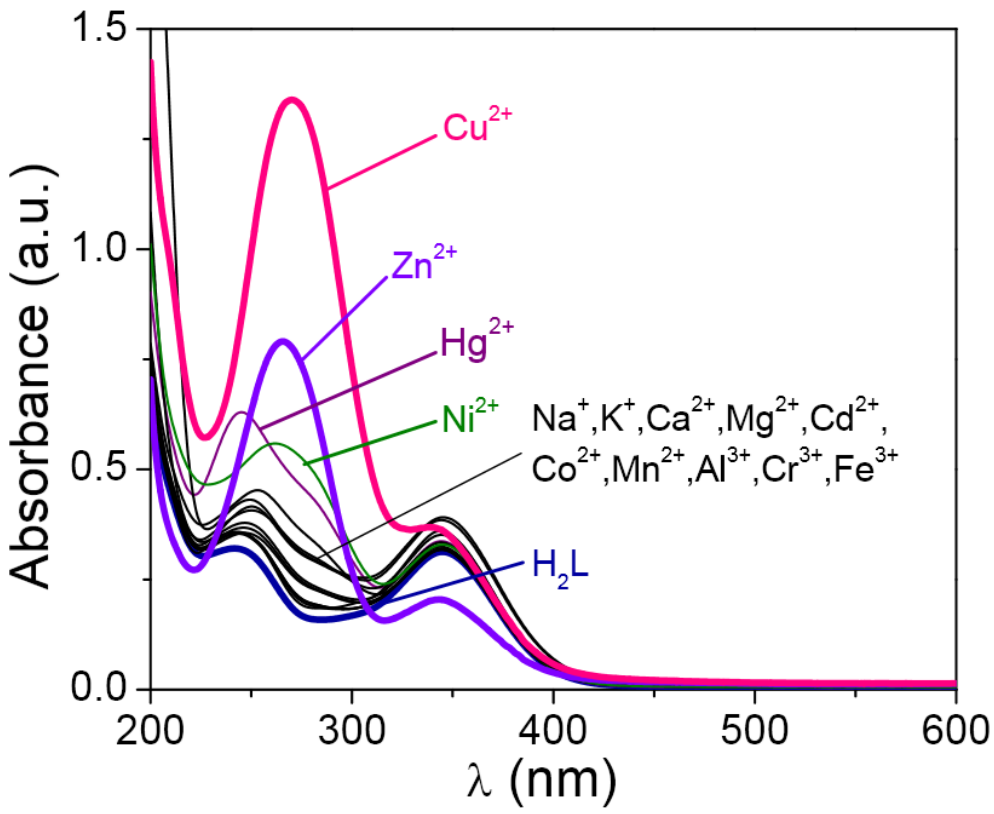

Fig. S9. UV-Vis spectra of chemosensor (H_2L) (20 μM) upon addition of 2 equivalent of various metal ions i,e, Na^+, K^+, Ca^{2+}, Mg^{2+}, Mn^{2+}, Fe^{3+}, Cr^{3+}, Co^{2+}, Ni^{2+}, Cu^{2+}, Zn^{2+}, Cd^{2+} and Hg^2 (40 μM)

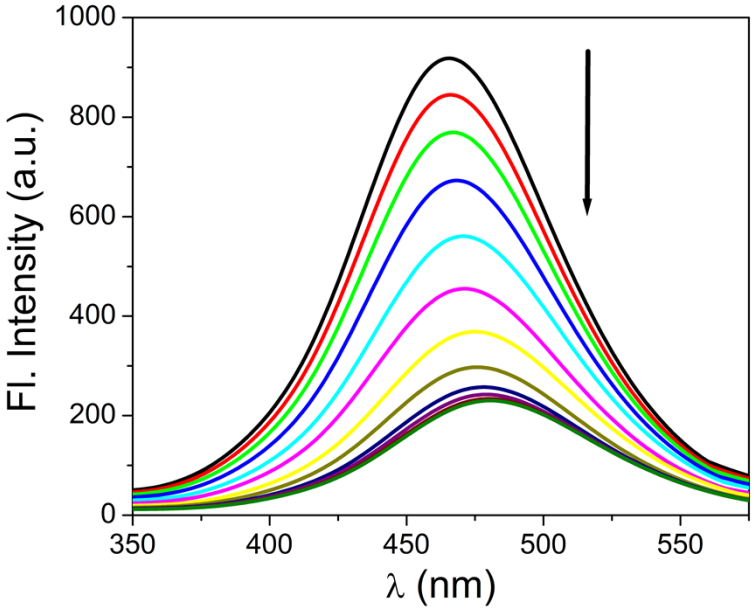

Fig. S10. Change in emission spectrum of H_2L-Zn^{2+} upon gradual addition of EDTA (40 μM) in 1:1, v/v CH_3CN:H_2O.

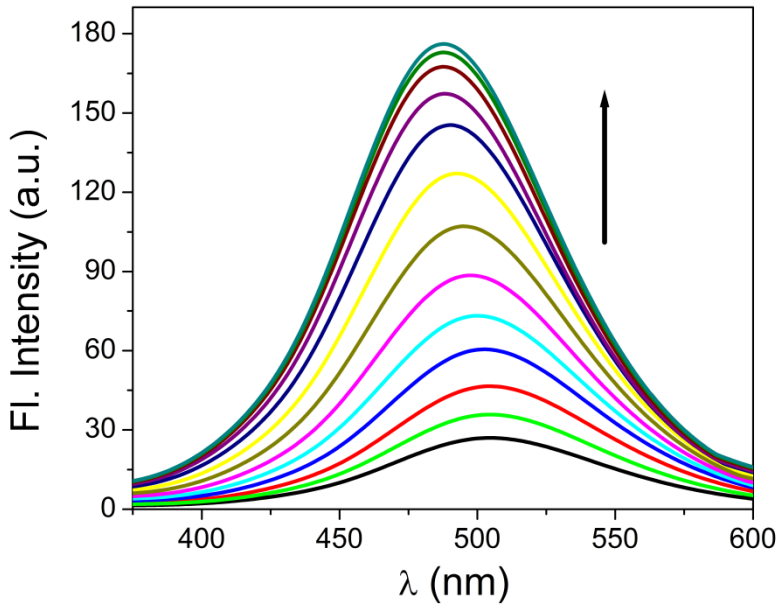

Fig. S11. Change in emission spectrum of H_2L-Cu^{2+} upon gradual addition of EDTA (40 μM) in 1:1, v/v CH_3CN:H_2O.

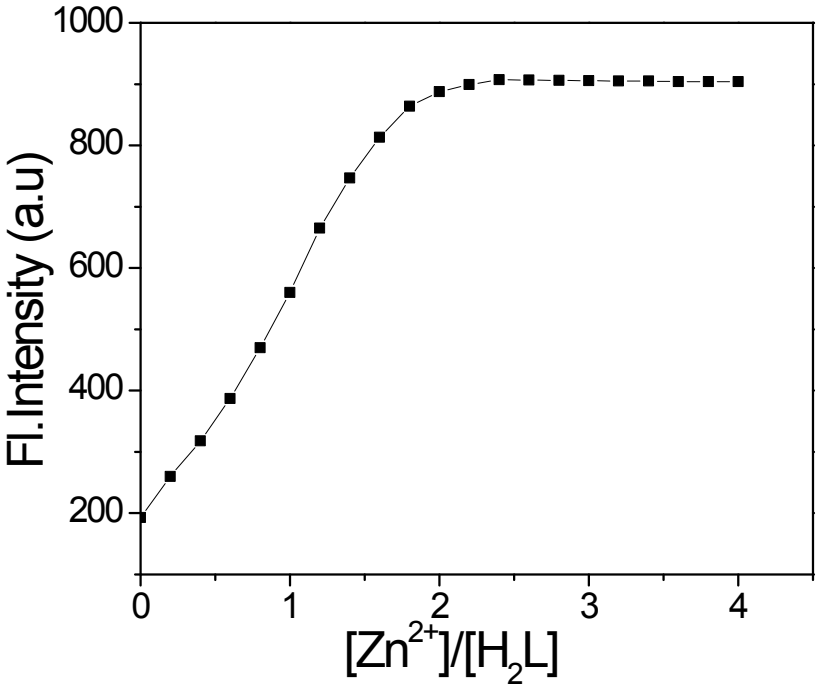

Fig. S12. Mole ratio plot of Zn^{2+} to the receptor H_2L

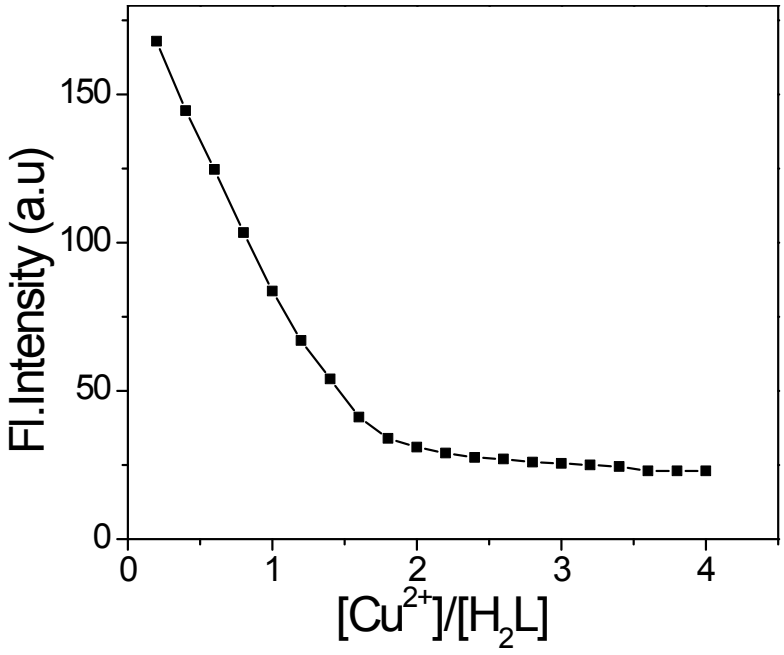

Fig. S13. Mole ratio plot of Cu^{2+} to the receptor H_2L

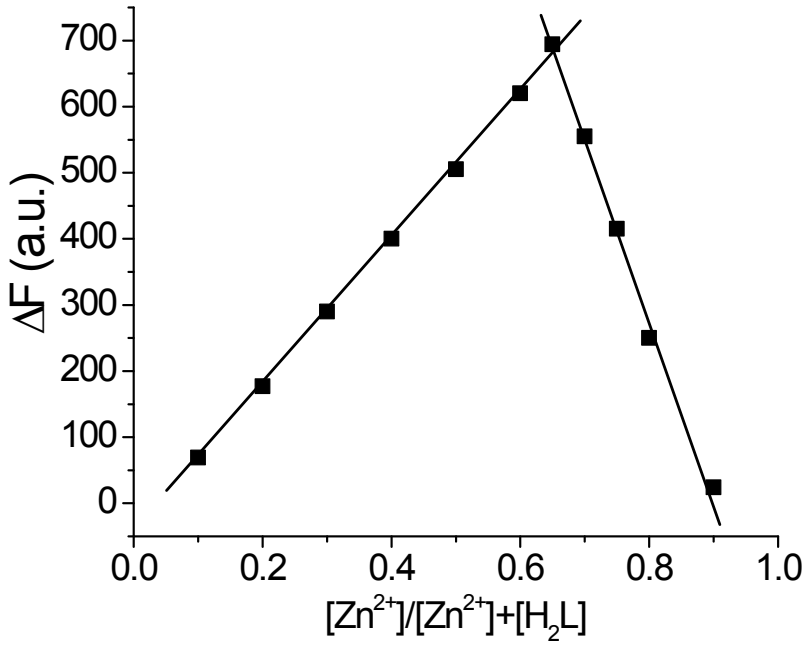

Fig. S14. Job's plot diagram of the receptor (H_2L) for Zn^{2+} (where ΔF indicates the change of emission intensity at 466 nm)

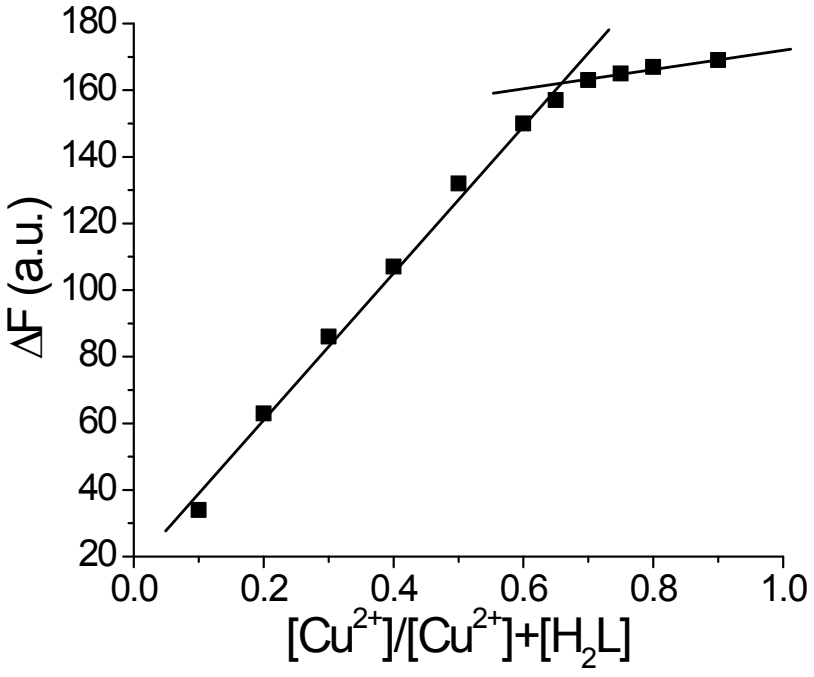

Fig. S15. Job's plot diagram of the receptor (H_2L) for Cu^{2+}

Determination of detection limit:

The detection limit was calculated based on the fluorescence titration. To determine the S/N ratio, the emission intensity of H_2L without any analyte was measured by 10 times and the standard deviation of blank measurements was found to be 2.6756×10^{-3}.

The limit of detection (LOD) of H_2L for Zn^{2+} and Cu^{2+} was determined from the following equation: LOD = K × σ Where K = 3 in this case and σ = $(Sb_1)/(S)$; Sb_1 is the standard deviation of the blank solution; S is the slope of the calibration curve.

From the linear response curve of H_2L for Zn^{2+} graph we get slope = 4.11821×10^{7}, Thus using the formula we get the LOD = 1.94×10^{-8} M.

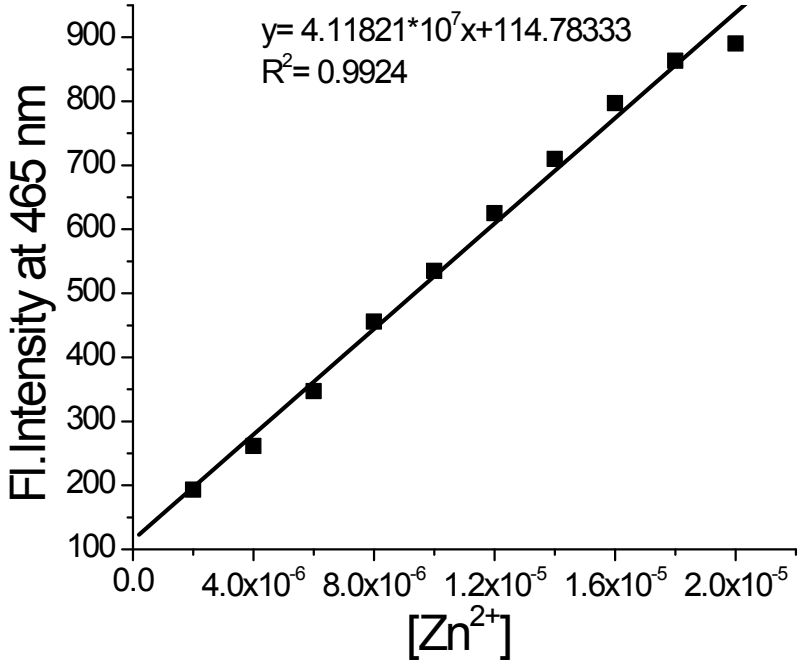

Fig. S16. Linear response curve of H_2L at 465 nm depending on the Zn^{2+}concentration.

From the linear response curve of H_2L for Zn^{2+} graph we get slope = -9.5×10^{6}, Thus using the formula we get the LOD = 1.87×10^{-9} M.

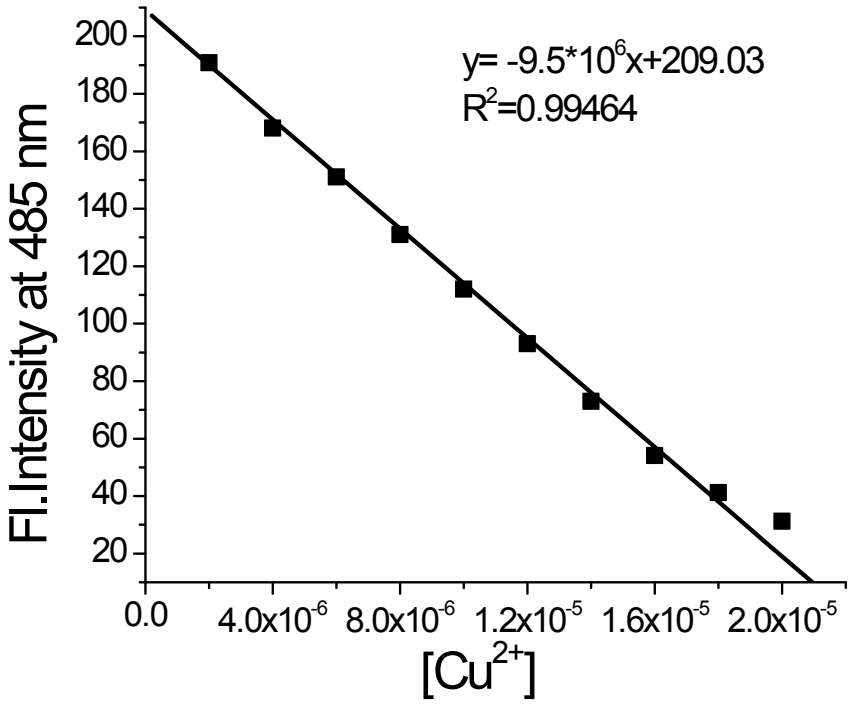

Fig. S17. Linear response curve of H_2L at 485 nm depending on the Cu^{2+}concentration.

Determination of binding constant from Fluorescence titration data:

Binding constant was calculated according to the Benesi-Hildebrand equation. K_a was calculated following the equation stated below.

$$1/(F-F_o) = 1/\{K_a(F_{max}–F_o)\ [M^{n+}]^x\} + 1/[F_{max}-F_o]$$

Here F_0, F and F_{max} indicate the emission in absence of, at intermediate and at infinite concentration of metal ion respectively. The binding constant K_a is determined from the ratio of intercept and slope of Benesi-Hildebrand plot. Plot of $1/[F-F_0]$ vs $1/[Zn^{2+}]^2$ gives a straight line indicating 1:2 complexation between H_2L and Zn^{2+}.

For the determination of binding constant of Cu^{2+} the equation modifies to

$$1/(F-F_o) = 1/\{K_a(F_{min}–F_o)\ [M^{n+}]^x\} + 1/[F_{min}-F_o]$$

Here F_0, F and F_{min} indicate the emission in absence of, at intermediate and at infinite concentration of metal ion respectively. The binding constant K_a is determined from the ratio of intercept and slope of Benesi-Hildebrand plot. Plot of $1/[F-F_0]$ vs $1/[Cu^{2+}]^2$ gives a straight line indicating 1:2 complexation between H_2L and Cu^{2+}.

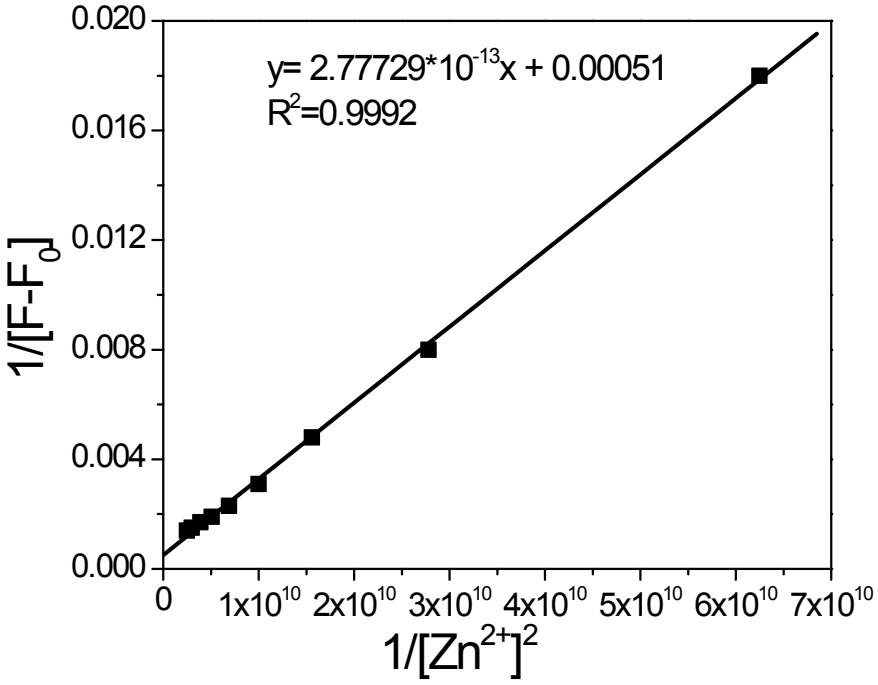

Fig. S18. Determination of association constant of H_2L for Zn^{2+} from fluorescent titration data

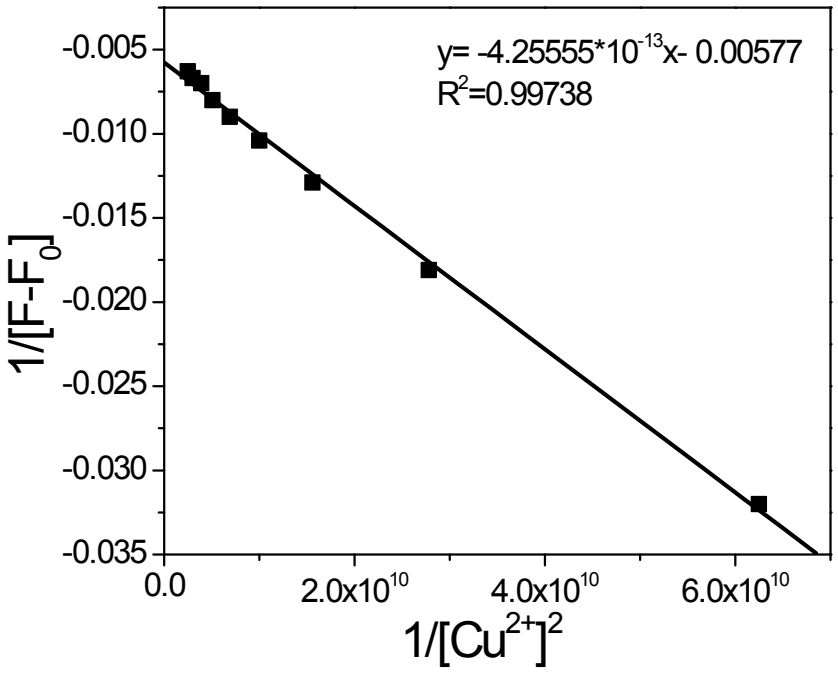

Fig. S19. Determination of association constant of H_2L for Cu^{2+} from fluorescent titration data

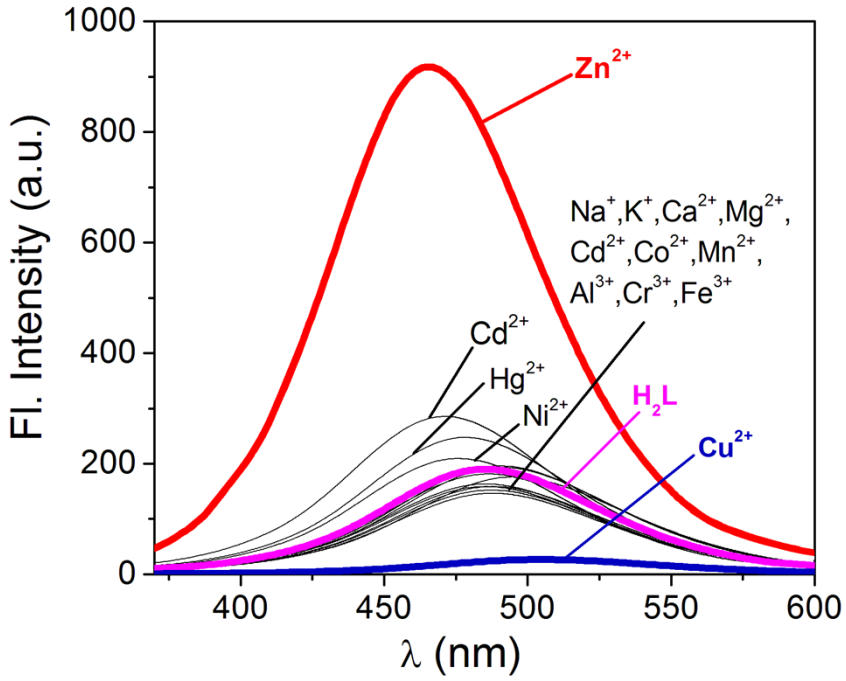

Fig. S20. Change in emission spectrum of H_2L (20 μM) upon addition of Na^+, K^+, Ca^{2+}, Mg^{2+}, Mn^{2+}, Fe^{3+}, Cr^{3+}, Al^{3+}, Co^{2+}, Ni^{2+}, Cu^{2+}, Zn^{2+}, Cd^{2+} and Hg^{2+} (40 μM) in CH_3CN:H_2O (1:1, v/v, pH=7.2).

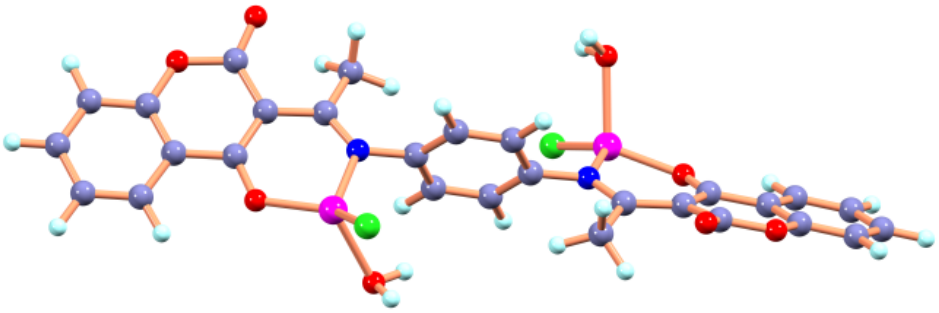

Fig. S21. Optimized structure of H_2L-Zn^{2+} complex by DFT/B3LYP/6-31G(d,p)/LANL2DZ method

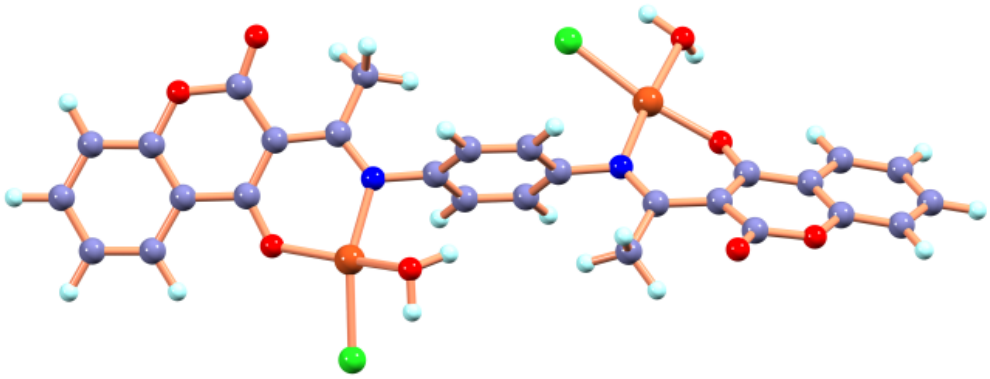

Fig. S22. Optimized structure of H_2L-Cu^{2+} complex by DFT/UB3LYP/6-31G(d,p)/LANL2DZ method

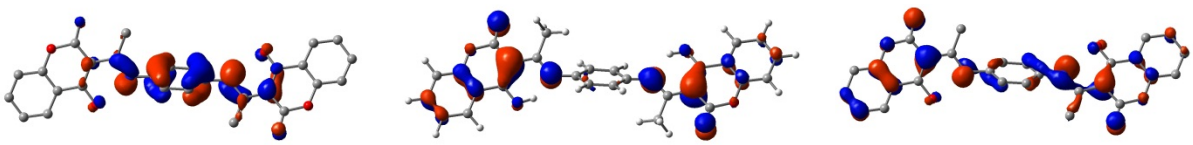

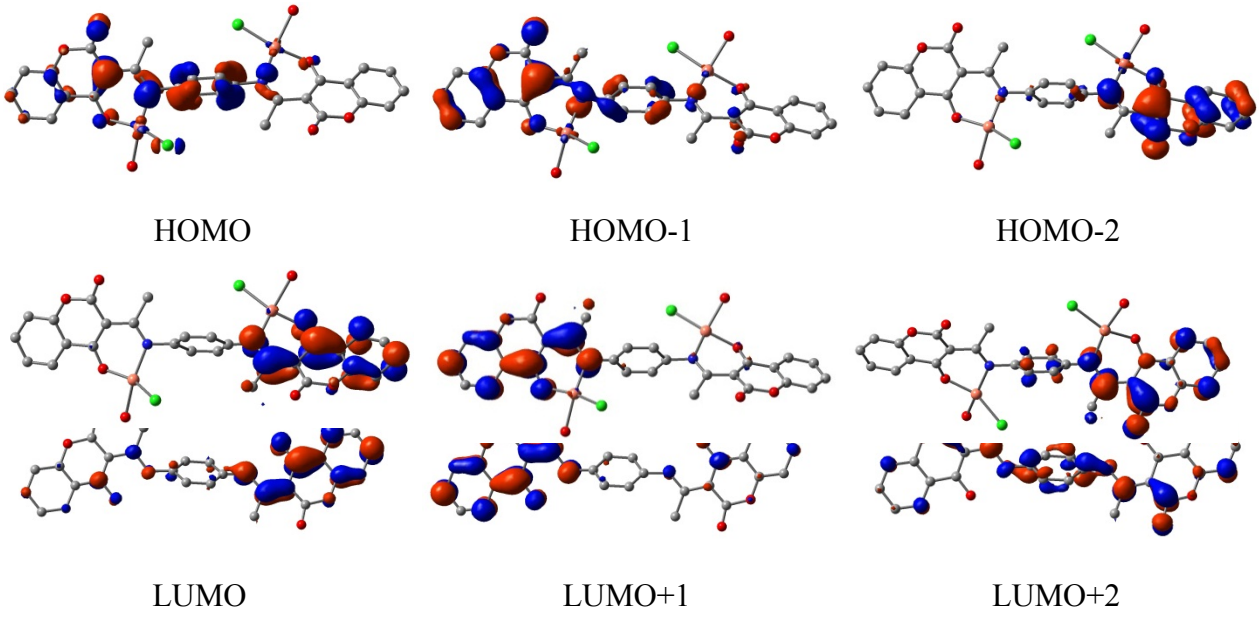

Fig. S23. Contour plots of some selected molecular orbitals of H_2L

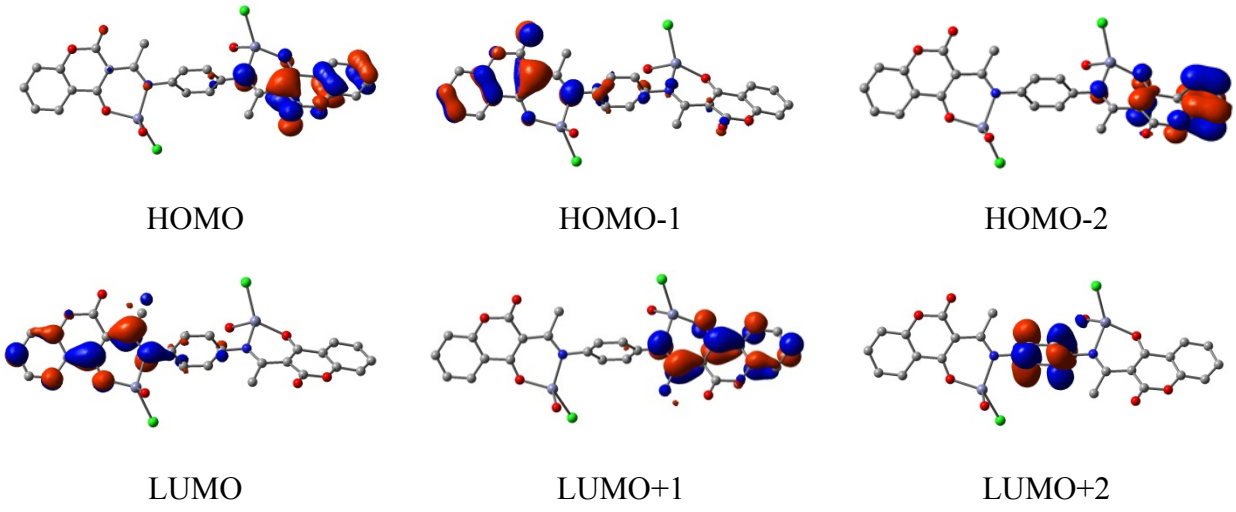

Fig. S24. Contour plots of some selected molecular orbitals of H_2L-Zn^{2+} complex

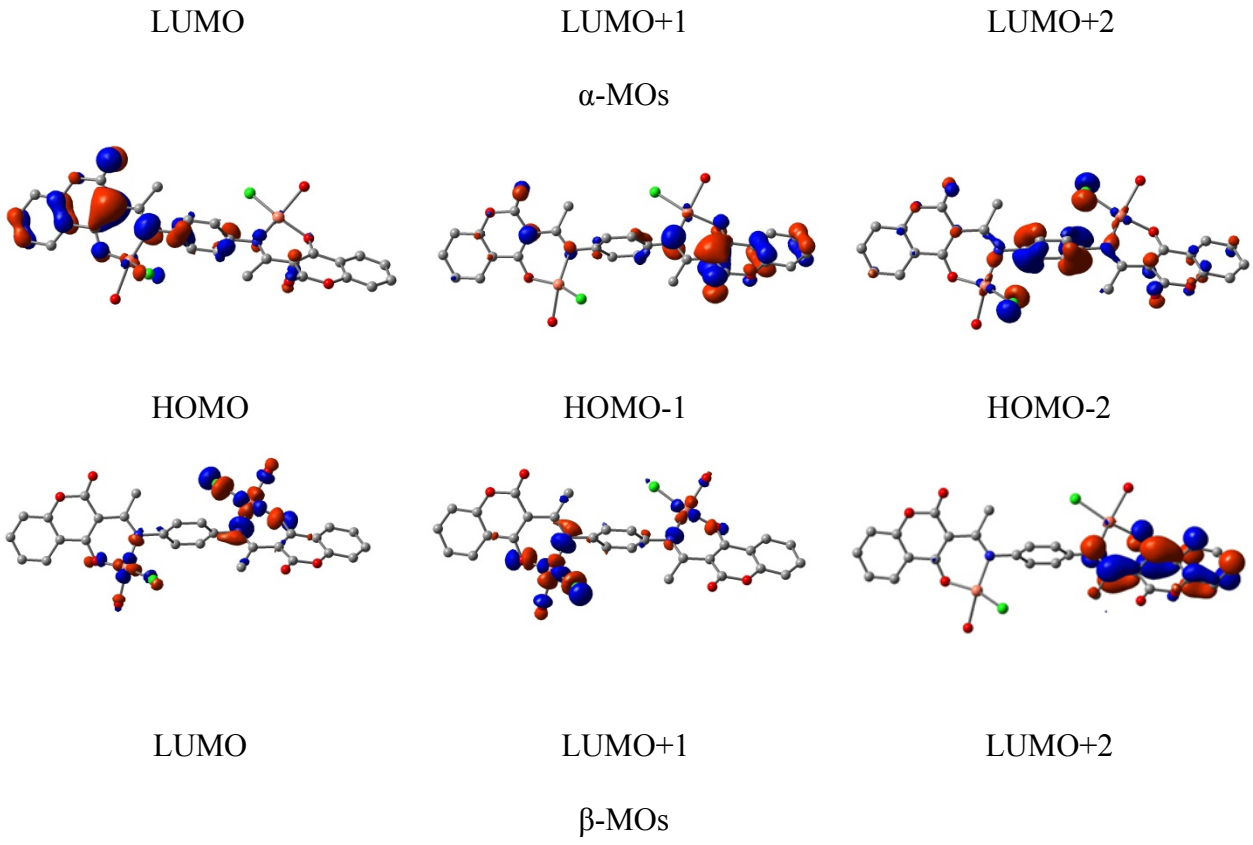

Fig. S25. Contour plots of some selected molecular orbitals of H_2L-Cu^{2+} complex

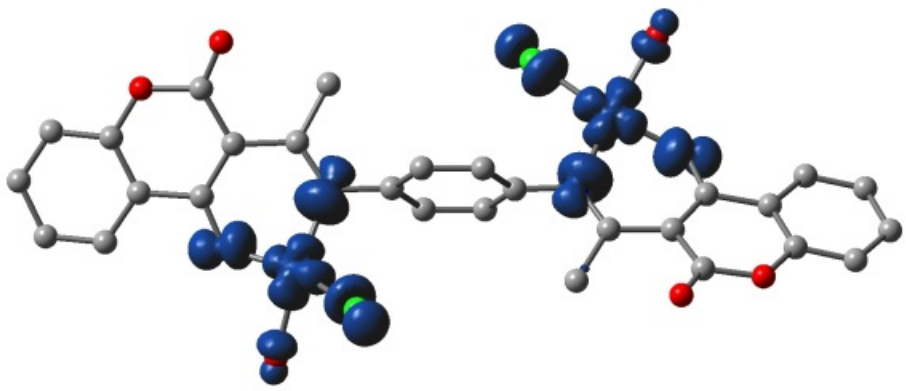

Fig. S26. Spin density plot of H_2L-Cu^{2+} complex

Table S1. Vertical electronic transitions calculated by TDDFT/B3LYP/CPCM method for chemosensor H_2L, H_2L-Zn^{2+} and H_2L-Cu^{2+} complexes

Compds.	$\lambda_{excitation}$ (nm)	Osc. Strength (f)	Key transition	Character
H_2L	338.4	0.7214	HOMO $\rightarrow$ LUMO	ILCT
H_2L-Zn^{2+}	340.2	0.6960	HOMO $\rightarrow$ LUMO	ILCT
H_2L-Cu^{2+}	482.0	0.0175	HOMO(β) $\rightarrow$ LUMO+1(β) HOMO(β) $\rightarrow$ LUMO(β)	LMCT
	358.9	0.2016	HOMO-1(β) $\rightarrow$ LUMO+2(β)	ILCT